AGU PUBLICATIONS

JGR

Journal of Geophysical Research: Oceans

RESEARCH ARTICLE

10.1002/2014JC010261

Key Points:
- Permafrost OC settles rapidly, undergoes little degradation, and dominates sediments
- Contemporary terrestrial OC remains in suspension and is actively degraded
- Marine OC is subject to vertical transport and is actively degraded

Supporting Information:
- Readme
- Supplementary material

Correspondence to:
J. E. Vonk,
j.e.vonk@uu.nl

Citation:
Vonk, J. E., I. P. Semiletov, O. V. Dudarev, T. I. Eglinton, A. Andersson, N. Shakhova, A. Charkin, B. Heim, and Ö. Gustafsson (2014), Preferential burial of permafrost-derived organic carbon in Siberian-Arctic shelf waters, *J. Geophys. Res. Oceans*, *119*, 8410–8421, doi:10.1002/2014JC010261.

Received 21 JUN 2014
Accepted 17 NOV 2014
Accepted article online 21 NOV 2014
Published online 5 DEC 2014

Preferential burial of permafrost-derived organic carbon in Siberian-Arctic shelf waters

Jorien E. Vonk[1,2,3], Igor P. Semiletov[4,5,6], Oleg V. Dudarev[4], Timothy I. Eglinton[2], August Andersson[1], Natalia Shakhova[4,5,6], Alexander Charkin[4,6], Birgit Heim[7], and Örjan Gustafsson[1]

[1]Department of Applied Environmental Science and Bolin Centre for Climate Research, Stockholm University, Stockholm, Sweden, [2]Swiss Federal Institute of Technology (ETH), Geological Institute, Zürich, Switzerland, [3]Department of Earth Sciences, Utrecht University, Utrecht, The Netherlands, [4]Pacific Oceanological Institute, Far Eastern Branch, Russian Academy of Sciences, Vladivostok, Russia, [5]International Arctic Research Center, University of Alaska Fairbanks, Fairbanks, Alaska, USA, [6]National Research Tomsk Polytechnic University, Tomsk, Russia, [7]Alfred-Wegener-Institut Helmholtz-Zentrum für Polar- und Meeresforschung, Periglacial Research Group, Potsdam, Germany

Abstract The rapidly changing East Siberian Arctic Shelf (ESAS) receives large amounts of terrestrial organic carbon (OC) from coastal erosion and Russian-Arctic rivers. Climate warming increases thawing of coastal Ice Complex Deposits (ICD) and can change both the amount of released OC, as well as its propensity to be converted to greenhouse gases (fueling further global warming) or to be buried in coastal sediments. This study aimed to unravel the susceptibility to degradation, and transport and dispersal patterns of OC delivered to the ESAS. Bulk and molecular radiocarbon analyses on surface particulate matter (PM), sinking PM and underlying surface sediments illustrate the active release of old OC from coastal permafrost. Molecular tracers for recalcitrant soil OC showed ages of 3.4–13 ^{14}C-ky in surface PM and 5.5–18 ^{14}C-ky in surface sediments. The age difference of these markers between surface PM and surface sediments is larger (i) in regions with low OC accumulation rates, suggesting a weaker exchange between water column and sediments, and (ii) with increasing distance from the Lena River, suggesting preferential settling of fluvially derived old OC nearshore. A dual-carbon end-member mixing model showed that (i) contemporary terrestrial OC is dispersed mainly by horizontal transport while being subject to active degradation, (ii) marine OC is most affected by vertical transport and also actively degraded in the water column, and (iii) OC from ICD settles rapidly and dominates surface sediments. Preferential burial of ICD-OC released into ESAS coastal waters might therefore lower the suggested carbon cycle climate feedback from thawing ICD permafrost.

1. Introduction

Arctic regions warm more rapidly than other places on Earth [e.g., *IPCC*, 2013; *Jeffries et al*., 2013] which has in recent decades led to a diminishing sea ice cover [*Cavalieri and Parkinson*, 2012], a longer melt season [*Stroeve et al*., 2014], increasing base flow in Eurasian Arctic rivers [*Smith et al*., 2007], increased storminess [*Francis et al*., 2011], and widespread thaw of onshore and offshore permafrost [*Jorgenson et al*., 2006; *Nicolsky et al*., 2012; *Shakhova et al*., 2014]. These changes will likely change the fate and degradation of carbon that is now mobilized from permafrost, perennially frozen soils that store about twice as much carbon as is currently in the atmosphere [*Tarnocai et al*., 2009; *Hugelius et al*., 2014]. Coastal waters of the East Siberian Arctic Shelf (ESAS) are dominated by terrestrial organic carbon (OC) that is mostly delivered by rivers and coastal erosion [*Vonk et al*., 2010b, 2012]. Coastlines that consist of Ice Complex deposits (ICD)—ice-rich Pleistocene permafrost (or "yedoma") [*Zimov et al*., 2006]—are particularly vulnerable to erosion, with erosion rates 5–7 times higher than other permafrost coasts [*Grigoriev et al*., 2004]. The propensity of thawed permafrost OC to be either transformed into greenhouse gases (CO_2, CH_4), or buried for long-term storage in coastal shelf/slope sediments is of key importance in terms of global climate-carbon feedbacks.

Previous geochemical work in this region has shown that despite shallow water depths (10–40m), surface sediment OC in the coastal ESAS is very different from surface particulate OC [*Karlsson et al*., 2011; *Vonk et al*., 2010b]. Surface sediment OC is old (Δ^{14}C between −424‰ and −622‰, corresponding to 4500–7800 ^{14}C-yrs) and relatively fresh (as indicated by molecular degradation proxies), whereas surface particulate OC is younger (−16 to −374‰, 100–3700 ^{14}C-yrs) and appears more degraded. Substantial degradation of

particulate OC (2.5 ± 1.6 Tg/yr in ESAS) [*Sánchez-García et al*., 2011] is an important contributor to the observed regional supersaturation of CO_2 [*Semiletov*, 1999a, 2013; *Pipko et al*., 2005, 2011]. Meanwhile, sedimentation of particulate OC in the ESAS is estimated to be between 1.4 Tg/yr (Holocene estimates) [*Stein and Macdonald*, 2004] and 20 ± 8 Tg/yr (current burial rate, only OC from ICD) [*Vonk et al*., 2012]. Coastal sedimentation processes here largely depend on river discharge and sea-ice regime, giving rise to a large interannual, seasonal, and spatial variability [*Charkin et al*., 2011; *Wegner et al*., 2013].

The propensity of (particulate) OC toward degradation and/or sedimentation is not just determined by its chemical structure, but also by the extent of physical association of OC to mineral surfaces [*Keil et al*., 1994; *Huguet et al*., 2008]. Organic matter-mineral interactions protect the organic matter from degradation and ballast the material for rapid settling. These interactions largely control OC burial and preservation [*Hedges et al*., 1997]. Here, they are likely a key factor in determining the nature and extent of climate-carbon feedbacks as terrestrial OC fluxes into the ESAS continue to increase.

Compound-specific radiocarbon analysis [*Eglinton et al*., 1996] has proven to be a powerful tool to deconvolute OC sources and unravel terrestrial carbon transport pathways and ages [e.g., *Gustafsson et al*., 2011; *Feng et al*., 2013]. Long-chain *n*-alkanoic acids [*Eglinton and Hamilton*, 1967] originate from epicuticular leaf waxes and are commonly used as tracers for recalcitrant soil OM [*Drenzek et al*., 2007; *Vonk et al*., 2010a]. We have performed molecular ^{14}C analyses on long-chain *n*-alkanoic acids in both surface water particles and surface sediments from key locations in the ESAS that were collected during the period of maximum seasonal permafrost thaw in late August. We also deployed sediment traps at these sites in order to collect sinking particles, serving as the intermediate between surface water and sediment OM pools, that were analyzed for bulk geochemical and isotopic (stable and radiocarbon) OM composition. This combination of analyses provides new insights into the fate of OM, and specifically (i) its susceptibility to degradation versus burial, (ii) transformations during water column transport, and (iii) dispersal patterns (i.e., settling versus horizontal transport).

2. Study Area

The expansive ESAS (~1800 × 10^3 km^2) is the largest shelf system in the Arctic Ocean, consisting of the Laptev Sea, East Siberian Sea, and the western part of the Chukchi Sea. The region is ice-covered 9–11 months a year, but in recent decades the ice-free season is lengthening (2–3 days/decade earlier melt onset, 6–8 days/decade later freeze-up; *Stroeve et al*. 2014]. The shelf is very shallow (average water depth <50m) receives large freshwater inputs from several major Russian Arctic rivers draining into the ESAS (Khatanga, Lena, Yana, Indigirka, Kolyma) and is bordered by several thousand kilometers of actively eroding coastal cliffs [*Lantuit et al*. 2011; *Günther et al*. 2013]. Terrestrial OC input therefore dominates the system. Recent sedimentation rates are estimated to be between 0.11 and 0.16 cm/yr (n=3) and OC accumulation rates between 8 and 130 gOC/m^2/yr (n=13, mean ±95% confidence interval 36 ± 17 gOC/m^2/yr) [*Vonk et al*., 2012]. Total annual river OC fluxes are estimated to be ~9 Tg [*Stein and Macdonald*, 2004] with the Lena River being the largest (delivering ~5.7 Tg/yr as dissolved OC, *Holmes et al*. [2012]; and ~1.2 Tg/yr as particulate OC, *Rachold and Hubberten* [1999]). Coastal erosion rates vary from 0.5 to 10 m/y with regional maxima up to 20 m/yr [*Grigoriev*, 1993; *Rachold et al*. 2004; *Lantuit et al*. 2011, 2012; *Günther et al*. 2013]. Terrestrial OC input from coastal erosion is estimated to be between 4 [*Grigoriev et al*. 2004] and 11 Tg/yr [*Vonk et al*. 2012], dominating the sedimentary OC in the ESAS (46–92%) [*Vonk et al*., 2012; *Semiletov et al*., 1999b; 2012]. There is a prevailing eastward current along the coast [*Steele and Ermold*, 2004], transporting Lena River water through the Dmitry Laptev Strait into the East Siberian Sea.

3. Methods

3.1. Sampling

Samples were collected during the International Siberian Shelf Study (ISSS-08, Figure 1a) in August–September 2008 [*Semiletov and Gustafsson*, 2009]. Surface sediments were obtained with a van Veen grab sampler. With stainless steel spatulas, we manually transferred the upper 0–2 cm into polyethylene containers that were frozen immediately afterward. Sinking particulate matter was collected with a cylindrical sediment trap system [*Gustafsson et al*., 2004, 2013] that was bottom anchored with ~40 kg railway tracks and galvanized chains. The trap (one array per mooring) consisted of three PVC cylinders each holding a straight cylindrical glass tube (500 × 100 mm) and was positioned at 6–10 m water depth (YS-4 at 22 m), below the mixed

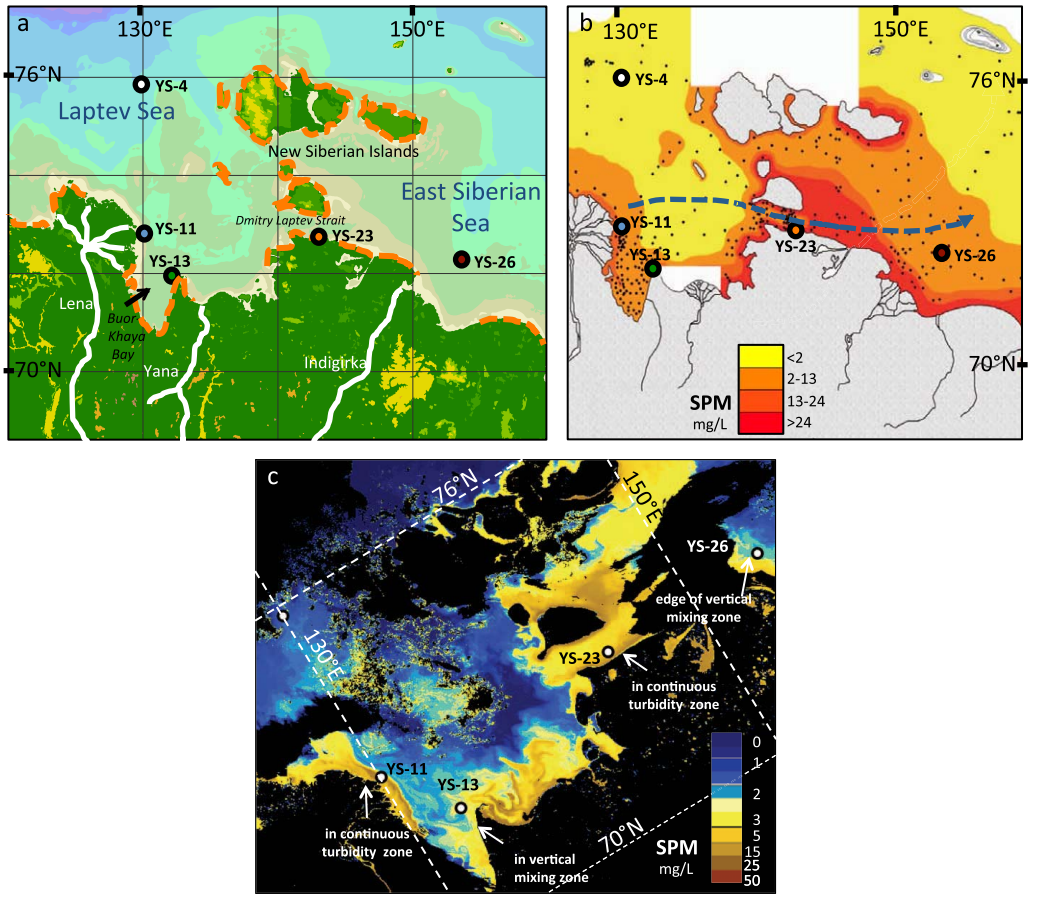

Figure 1. Map of study area (a) with study sites YS-4, YS-11, YS-13, YS-23, and YS-26, major rivers outlined, and active coastal erosion regions (coastline marked with orange-dashed line) [*Lantuit et al.*, 2011], and (b) contour map of surface particulate matter concentrations (mg/L) collected over 2003–2010 (all data points given in black) with dominant coastal current direction (blue-dashed line) [*Steele and Ermold*, 2004], and (c) processed MERIS Laptev Sea acquisition on 12 August 2008 with color-coded map of C2R_SPM, with land, detected clouds, and sea ice masked in black, and descriptions of prevailing hydrographical settings at the sampled stations (based on long-term 2006–2011 MERIS image analysis).

surface layer (5–9 m deep), and as far above the bottom (4–9 m) as possible (Table 1 and supporting information Figure S1). A small buoy was attached 3 m above the array to lift the mooring line. At the surface, a large spherical buoy was connected with a 10 m line to a flag buoy to minimize the effect of short-period wave motion. Recovered sediment trap glass tubes were allowed to settle for ~1 h. The overlying water was siphoned off, any visible swimmers were picked with long stainless steel forceps, and the water was transferred to 1000 mL polycarbonate bottles and frozen. We avoided using brines or poison to minimize zooplankton herniation [e.g., *Peterson and Dam*, 1990] and solubilization of POC into dissolved OC [e.g., *Hansell and Newton*, 1994]. Deployments were between 7 and 54 h (the cruise track did not allow for revisits).

Surface water POC for bulk geochemistry was collected in small volumes (1–3 L) from the middle of the surface mixed layer (between 2 and 4 m) with a rosette of Niskin bottles arranged around a Seabird CTD sensor package. Samples were filtered with an all-glass filtration set-up and precombusted 0.7 μm GF/F, further details in *Sánchez-García et al.*, [2011]. Surface water POC for compound-specific radiocarbon analyses was collected in large volumes (791L YS-11, 2101L YS-12, 1489L YS-23, and 3783L YS-26) also from the middle of the surface-mixed layer (between 2 and 4 m) with a submersible pump (model AN19, Debe Pumpar AB, Sweden) connected with reinforced silicon and PVC tubing to a stainless-steel/silicon-sealed filtration system, consisting of two 293 mm stainless steel filter towers holding precombusted 0.7 μm GF/F.

3.2. Bulk Elemental and Isotope Analyses

Bulk elemental (organic carbon, total nitrogen), $\delta^{13}C$ and $\Delta^{14}C$ analyses were performed according to procedures described previously [*Vonk et al.*, 2010a, 2010b; *Sánchez-García et al.*, 2011]. Bulk radiocarbon

Table 1. Sampling Information and Bulk and Molecular Geochemistry Results for Surface Water Particulate Matter, Sinking Particulate Matter and Surface Sediment in the Laptev and East Siberian Sea[a]

	Coordinates		Depth	Date[b]	TOC[c]	TOC/TN[d]	$\delta^{13}C$[e]	$\Delta^{14}C \pm$s.d.[f]	^{14}Cage $\pm$s.d.	$\Delta^{14}C \pm$s.d.[g]	^{14}Cage $\pm$s.d.
Station	°N	°E	m	(Time Deployed)	mg/g		‰	‰	yrs BP	‰	yrs BP
Surface water particulate matter									Bulk	*n*-Alkanoic Acids	
YS-4	75.99	129.98	Surface	24 Aug. 2008	87	9.2	−30.2	–	–	–	–
YS-11	73.02	129.99	Surface	25 Aug. 2008	842	8.5	−28.0	−202 ± 3	1750 ± 35	−452 ± 13 (43)	4,79 0 ±20
YS-13[h]	71.97	131.70	Surface	26 Aug. 2008	257	7.0	−32.0	−15.9 ± 6	75 ± 45	−594 ± 2 (77)	7180 ± 420
YS-23	72.79	142.67	Surface	30 Aug. 2008	165	5.8	−29.3	−517±3[i]	5,800 ± 50	−801 ± 3[i] (14/42)	12,950 ± 130
YS-26	72.46	150.60	Surface	31 Aug. 2008	61	4.5	−30.1	−408 ± 3[i]	4,155 ± 45	−351 ± 10[i] (13)	3,410 ± 130
Sinking particulate matter									Bulk	*n*-Alkanoic Acids	
YS-4	75.99	129.98	22	24 Aug. 2008 (11.5 h)	6.9	6.9	−27.1	−76 ± 10	575 ± 90	–	–
YS-11	73.02	129.99	7	25 Aug. 2008 (8 h)	20	9.3	−26.6	−390 ± 2	3,920 ± 20	–	–
YS-13	71.97	131.70	10	26 Aug. 2008 (54 h)	40	10	−28.8	−157 ± 3	1,315 ± 25	–	–
YS-23	72.79	142.67	6	30 Aug. 2008 (13 h)	26	8.3	−27.2	−450 ± 2	4,745 ± 20	–	–
YS-26	72.46	150.60	8	31 Aug. 2008 (7 h)	8.9	7.2	−26.9	−289 ± 9	26,85 ± 110	–	–
Surface sediment[j]									Bulk	*n*-Alkanoic Acids	
YS-4	75.99	129.98	50	24 Aug. 2008	13	8.0	−24.3	−437 ± 2[i]	4,550 ± 35	–	–
YS-11	71.96	129.54	11	25 Aug. 2008	4.8	14	−25.0	−609 ± 3	7,500 ± 60	−500 ± 5 (>10)	5,520 ± 95
YS-13	71.97	131.70	19	26 Aug. 2008	19	11	−25.9	−543 ± 2[i]	6,225 ± 35	−707 ± 40[i] (7)	9,805 ± 1,200
YS-23	72.79	142.67	10	30 Aug. 2008	9.1±1.5	8.9	−27.2 ± 0.1	−716 ± 2	10,050 ± 40	−895 ± 2[i] (15/47)	18,050 ± 170
YS-26	72.46	150.60	16	31 Aug. 2008	8.7 ± 0.2	8.4	−27.4 ± 0.1	−741 ± 1[i]	10,800 ± 45	−830 ± 5[i] (14)	14,200 ± 250

[a]The ^{13}C and ^{14}C results are given in ‰ measured relatively to VPDB and NBS oxalic acid, respectively. Standard deviations (s.d.) are reported when available.
[b]Total deployment time (hours) indicated between brackets for sinking particulate matter.
[c]Total Organic Carbon (TOC); surface particulate matter in μg/L, YS-11, YS-13 from *Karlsson et al.* [2011], YS-4, YS-23, and YS-26 from *Sánchez-García et al.* [2011]; sediment data from *Vonk et al.* [2012], *Gustafsson et al.* [2011] (YS-11).
[d]Total Nitrogen (TN); surface particulate matter (YS-11, YS-13 from *Karlsson et al.* [2011]; YS-4, YS-23, YS-26 from *Sánchez-García et al.* [2011]; sediment data from *Vonk et al.* [2012].
[e]$\delta^{13}C$ given in ‰ measured relatively to VPDB (surface particulate matter YS-11, YS-13 from *Karlsson et al.* [2011]; YS-4, YS-23, YS-26 from *Sánchez-García et al.* [2011]/sediment data from *Vonk et al.* [2012], *Gustafsson et al.* [2011] (YS-11).
[f]$\Delta^{14}C$ given in ‰ measured relatively to NBS oxalic acid.
[g]The ^{14}C results for *n*−alkanoic methyl esters (sum of C_{24}, C_{26}, and C_{28}) were corrected for measured ^{14}C values of the methyl group from the derivatization agent (BF_3-methanol) to obtain the inherent ^{14}C value for *n*-alkanoic acids.
[h]^{14}C analyses on *n*-alkanoic acids were performed on filters collected at nearby station YS-12 (71.92°N, 132.39°E).
[i]Data measured at ETH, other data from NOSAMS (see methods). Sample size in μg C is reported in brackets. For YS-23 surface SPM and surface sediments, we performed duplicate ^{14}C measurements on samples with different sample size. Results shown are averages, duplicate $\Delta^{14}C$ values were <10‰ different.
[j]YS-4, YS-13, and YS-26 are sediment core tops (core 2A, 3B, and 1A, respectively), YS-11 and YS-23 are grab samples. YS-11 data are from *Gustafsson et al.* [2011].

measurements were done at the National Ocean Sciences Accelerator Mass Spectrometry (NOSAMS) facility of the Woods Hole Oceanographic Institution (WHOI; USA) and at the AMS facility of the Laboratory of Ion Beam Physics (LIP) of the Swiss Federal Institute of Technology (ETH-Zürich, Switzerland).

Surface sediments and filters were freeze-dried (Christ Alpha 2-4, LSC; Vacuum hybrid pump, Vacubrand RC-6; Martin Christ, Labex Instrument AB) and extracted and fractionated as described elsewhere [*Vonk et al.* 2010a]. The high-molecular weight (HMW) *n*-alkanoic acids were isolated with preparative capillary gas chromatography (pc-GC) and combined (C_{24}, C_{26}, and C_{28}). The isolated fractions were run on a GC-FID to detect impurities (all <5%). The compounds were transferred with dichloromethane to precombusted quartz-tubes, and gently evaporated under N_2. After addition of precombusted CuO, the tubes were flame-sealed under vacuum, combusted at 850°C for 5 h, and the resulting CO_2 was cryogenically purified and quantified before analysis on a miniaturized radiocarbon dating system (MICADAS) at LIP (ETH-Zürich). One batch of isolated *n*-alkanoic acids was directly sent to NOSAMS, where they were converted to CO_2, graphitized and analyzed on the AMS. The ^{14}C results for *n*-alkanoic methyl esters were corrected for measured ^{14}C values of the methyl group from the derivatization agent (BF3 in methanol) to obtain the inherent ^{14}C value for the *n*-alkanoic acids.

3.3. Ocean Color Remote Sensing

Ocean color remote sensing has the potential to provide mapped calculated optical aquatic parameters such as turbidity, transparency, and suspended matter loading. Since 2010, the CoastColour project (http://www.coastcolour.org/) of the European Space Agency (ESA) has incorporated the Kara Sea and Laptev Sea regions into its program for evaluating the applicability of ocean color remote sensing in Arctic coastal waters. With support of this program, the optical remote sensing parameters were calculated from time

series from 2006 to 2011 on the ocean color satellite sensor MERIS (Medium-Resolution Imaging Spectrometer) using a CoastColour processing method. The Case-2 Regional Processor module (C2R) [*Doerffer and Schiller*, 2007] installed in BEAM-VISAT (Brockmann Consult) was used to process the MERIS top-of-atmosphere radiances to obtain optical parameters and concentrations of chlorophyll, suspended matter (SPM), and colored dissolved organic matter with specific adaptions to the Laptev Sea according to *Örek et al*. [2013] and *Heim et al*. [2013].

Heim et al. [2013] derived a Laptev Sea satellite-derived SPM algorithm based on the strong relationship between the calculated MERIS-derived backscattering coefficient (bb_{spm}) and in situ SPM values from 2010: SPM (mg/L)$= 50.78 \times bb_{spm}$. The satellite-derived values (Figure 1c) coincide well with the long-term derived SPM concentrations based on in situ measurements (Figure 1b). The MERIS time series from 2007 to 2011 of mapped optical aquatic parameters during the ice-free season was used to understand the representativeness of the hydrographic setting of the stations YS-11, YS-13, YS-23, and YS-26 in August 2008 (Figure 1c). Specifically, a relatively cloud-free MERIS acquisition on 12 August 2008 (Figure 1c), 2 weeks prior to sampling was processed using the C2R processors and the Laptev Sea SPM algorithm.

3.4. End-Member Analysis and Monte Carlo Simulations

We applied a dual-carbon ($\delta^{13}C$ and $\Delta^{14}C$), three-source mixing model on the samples following the approach by *Vonk et al*. [2010b], *Karlsson et al*. [2011], and *Vonk et al*. [2012]. End-member values of marine OC and ICD-OC were identical to *Vonk et al*. [2012], being $\delta^{13}C$ $-24‰ \pm 1‰$ and $\Delta^{14}C$ $+60‰ \pm 60‰$ (marine OC) and $\delta^{13}C$ $-26.3‰ \pm 0.67‰$ and $\Delta^{14}C$ $-940‰ \pm 84‰$ (ICD-OC). The third end-member is defined as topsoil OC, which we visualize as OC from the active layer and fresh vegetation debris that is transported by rivers and coastal erosion to the shelf. We defined this as $\delta^{13}C$ $-28.8 \pm 2.7‰$ (n=33; based on 14 topsoil samples and 19 riverine particulate OC samples in the ESAS drainage basin; supporting information Table S2; *Tesi et al*. [2014]; *Sánchez-García et al*. [2014]) and $\Delta^{14}C$ $-179 \pm 128‰$ (n=25) based on riverine particulate OC values from sites not (or minimally) draining ICD soils along with surface soil samples bordering the Lena River and Lena Delta (supporting information Table S3; *Höfle et al*. [2013]; *Kuptsov and Lisitsin* [1996]). We have to note that OC from river plankton, with variable $\delta^{13}C$ values ($-31.0‰$, *Rachold and Hubberten* [1999]; $-23.3‰$ plankton bloom Pantaleikha River) also contributes to this end-member. *Kraberg et al*. [2013] estimated chlorophyll-a contributions in the Buor-Khaya Bay to be around 2 μg/L. *Sorokin and Sorokin* [1996] estimated total primary production in the Lena River (September 1991) to be between 50 and 162 μg C/L, which is 6–49% of the total POC at station YS-11 and YS-13 (842 and 257 μg C/L, respectively). This is likely at the high end of a potential plankton contribution as light penetration is lower (due to higher turbidities) during the rest of the summer.

To account for end-member variability in the source apportionment estimates, a Monte Carlo approach was implemented [*Sheesley et al*., 2011; *Andersson*, 2011]. Both the end-member values and data points were represented by normal distributions. The parameter values for the end-members are outlined above, and the standard deviations for the data points were uniformly assigned to $50‰$ in the $\Delta^{14}C$ dimension and $0.5‰$ in the $\delta^{13}C$ dimension. The calculations were run using Matlab version 2013b (Mathworks Inc.). In total, 10^6 iterations were run for each sample, discarding fractional source contributions outside of the physical range ([0,1]).

4. Results and Discussion

A shift in bulk geochemical properties from surface waters to surface sediments suggests ongoing degradation in the water column. In August 2008, surface waters in the ESAS show clear regional geographic maxima in particulate matter loading (Figures 1b and 1c) and turbidity (supporting information Figure S1) in the near shore areas surrounding the Lena River delta, east of the Buor-Khaya Cape in the Yana Bay, and most distinctly in the shallow Dmitry Laptev Strait/New Siberian Island region. This suggests the active release and suspension of organic matter from rivers and coastal/sea floor erosion. At stations YS-23 and YS-26, distal from major river inflow, the stratification is weak, whereas the water column at YS-11 and YS-13 in the Buor-Khaya Bay appears highly stratified (supporting information Figure S1). The Buor-Khaya Bay is not always stratified, but in August 2008 an anomalously large Lena discharge (1999–2007 August average 27,500 m^3/s, 2008 August 35,000 m^3/s; ArcticRIMS Project http://rims.unh.edu) and relatively low wind conditions, led to strong stratification resulting in an accumulation-sedimentation regime [*Charkin et al*., 2011]

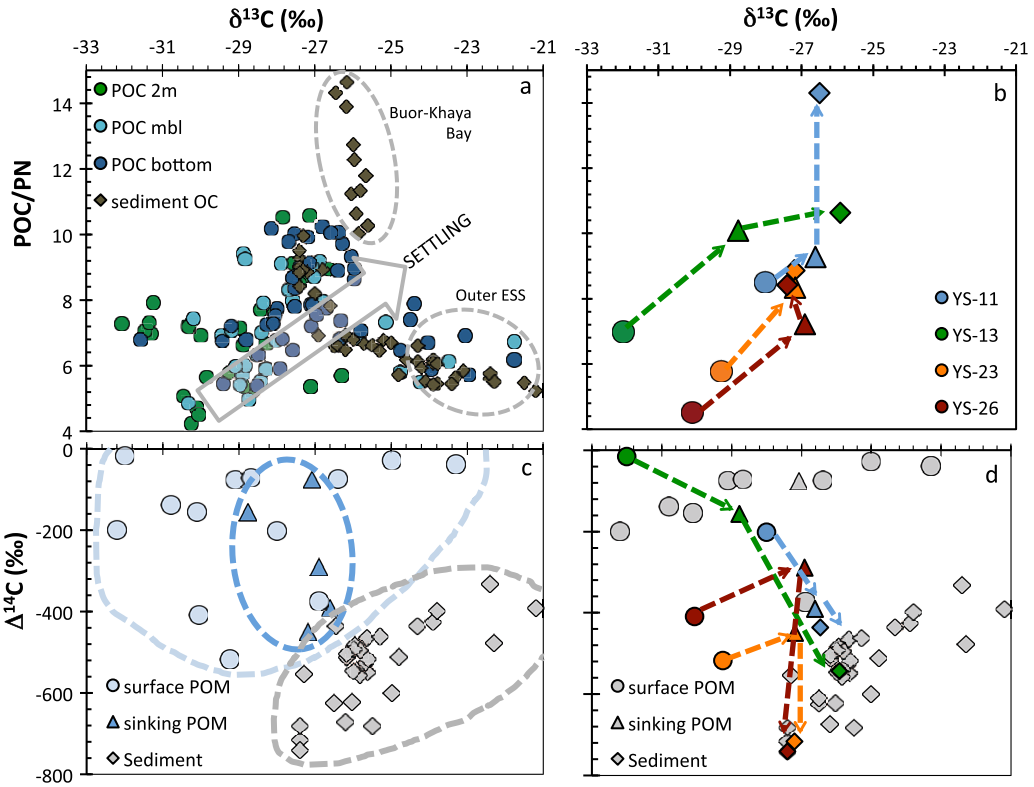

Figure 2. Bulk geochemical properties of particulate organic carbon (POC) and sediment OC for the ESAS in 2008. With total particulate organic carbon (POC) to total particulate nitrogen (PN) ratios against $\delta^{13}C$ (‰) for (a) surface POC (2m depth; green circles), middle bottom layer POC (mbl, between bottom and pycnocline; light blue circles), bottom POC (dark blue circles), and sediment OC (brown diamonds), all POC and sediment OC have previously been published [*Sánchez-García et al.* 2011; *Karlsson et al.* 2011; *Vonk et al.*, 2012]. (b) Surface POC (circles), sinking POC (triangles), and sediment OC (diamonds) are given for YS-11 (blue), YS-13 (green), YS-23 (orange), and YS-26 (red). Then, $\Delta^{14}C$ (‰) against $\delta^{13}C$ (‰) for (c) all surface POC (circles) [*Karlsson et al.*, 2011; *Vonk et al.*, 2010b], sinking POC (triangles), and sediment OC (diamonds) [*Vonk et al.*, 2012], and (d) same as (c) but with color coding for target sites YS-11 (blue), YS-13 (green), YS-23 (orange), and YS-26 (red). Arrows indicate the direction of flow from surface POC to sinking POC to sediment OC.

that generally only otherwise occurs when the bay is ice covered. Likely, this also minimized the resuspension of bottom sediments. Atmospheric conditions over the Laptev Sea in August 2008 were also anomalous [*Wegner et al.* 2013, *Heim et al.* 2013] with an anticyclonic atmospheric circulation pattern with dominating offshore winds instead of the normal cyclonic atmospheric circulation pattern. The Lena River freshwater layer reached up to a latitude of 76.8°N (North of the Lena River delta), and up to 77.8°N (North of the New Siberian Islands) [*Wegner et al.* 2013] and most of the Lena fresh water was transported Northward to the outer shelf, whereas the Eastern Siberian coastal jet developed only weakly in summer 2008. These anomalous hydrographic and atmospheric conditions will directly affect the distribution of organic matter in the water column and, more indirectly, also the underlying surface sediments. In general, one has to note that surface sediments represent a more integrated signal (likely over several seasons), whereas SPM represents a more short-term signal. Nevertheless, surface sediments are "downstream" in the transport-diagenesis continuum relative to the surface SPM and sinking SPM, and this allows us to assess effects of degradation and transport on OC that is released into the ESAS. Long-term MERIS time series analysis of all (partly) cloud-free images during summer months of 2006 through 2011 provide information of the typical hydrographical settings of the ISSS-08 stations. The images suggest that during late-summer (August) YS-11 and YS-23 are always within the intense turbidity zones (Figure 1c), whereas YS-13 is within reach of the lateral advection of material from the coast and YS-26 is on the edge of the turbidity front in deeper waters where the position of the front, and the influence of tidal energy, determines the enrichment with surface SPM.

During particle settling, the geochemical properties of OM seem to shift; TOC/TN ratios generally increase and $\delta^{13}C$ signatures become more enriched from surface SPM → middle bottom layer SPM → bottom SPM → sediment OM (Figure 2a), as well as from surface SPM → sinking SPM (sediment trap material) →

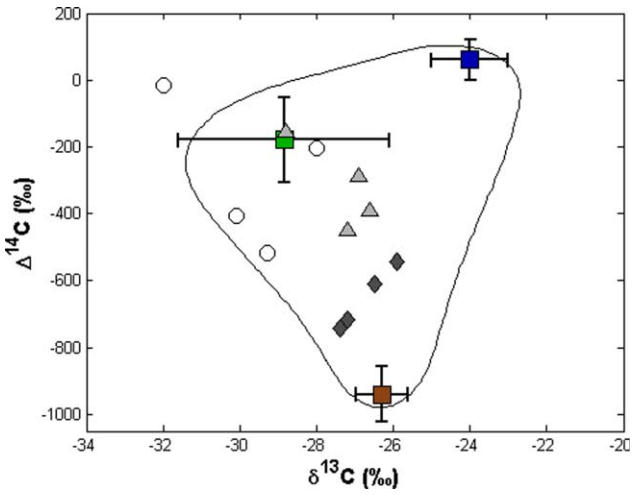

Figure 3. Surface particulate POC (circles), sinking POC (triangles), and sediment OC (diamonds) values of $\delta^{13}C$ and $\Delta^{14}C$, along with the end-members that are used for Monte Carlo source-apportionment; marine OC (blue rectangle; $\delta^{13}C$ $-24 \pm 1‰$ and $\Delta^{14}C$ $+60 \pm 60‰$; *Vonk et al.*, 2012], topsoil OC (green rectangle; $\delta^{13}C$ $-28.8 \pm 2.7‰$; $\Delta^{14}C$ $-179 \pm 128‰$; supporting information Tables S2 and S3), and ICD-OC (brown rectangle; $\delta^{13}C$ $-26.3 \pm 0.67‰$ and $\Delta^{14}C$ $-940 \pm 84‰$; *Vonk et al.*, 2012]. The solid line represents the 95% confidence interval region based on the three end-members and their uncertainty.

sediment OM (Figure 2b). This shift likely reflects a combination of (i) preferential degradation of fresh (most ^{13}C depleted) terrestrial OM, (ii) degradation of in situ produced river (autochthonous) OM (relatively low TOC/TN ratios, ^{13}C depleted), and/or (iii) degradation of marine OM (relatively low TOC/TN ratios, ^{13}C enriched). A settling-induced shift in $\delta^{13}C$ was also observed in *Waite et al.* [2005], suggesting changes in the phytoplankton community. The relative increase in $\delta^{13}C$ values from surface POC to sediment OC could, however, also suggest that ICD-OC ($\delta^{13}C$ end-member defined in *Vonk et al.* [2012] as $-26.3 \pm 0.67‰$) is more abundant in sediments, whereas fresh, contemporary "topsoil" OM (end-member $-28.8 \pm 2.7‰$) dominates in surface POC. There is, however, a bifurcation in the trend, that seems to be driven by spatial differences (Figure 2a and supporting information Figure S2); the highest TOC/TN ratios occur in the Buor-Khaya Bay while the lowest TOC/TN (in combination with higher $\delta^{13}C$ values) prevail in the outer/eastern East Siberian Sea and Chukchi Sea that are influenced more strongly by marine (Pacific) inflow.

The surface, sinking and sediment $\Delta^{14}C$ data together span a surprisingly wide range (Figures 2c and 2d), varying from contemporary values (some of the surface POC) to ages of more than 10,000 ^{14}C-years (surface sediment OC). This corroborates previous findings that report old ^{14}C ages of surface sediment OC relative to surface particulate OC [*Karlsson et al.*, 2011; *Vonk et al.*, 2010a, 2010b], and also suggests that ICD-OC ($\Delta^{14}C$ end-member $-940 \pm 84‰$, *Vonk et al.* [2012]) prevails in sediment OC compared to topsoil-OC ($-179 \pm 128‰$). The oldest surface POC ^{14}C values ($-374‰$ to $-518‰$) are measured near coastal erosion sites YS-23 and YS-26 and YS-14 [*Karlsson et al.*, 2011; near Muostakh Island), while the youngest values ($-16‰$ to $-37‰$) are found off the Kolyma coast [YS-37, YS-39; *Vonk et al.*, 2010b] and west of the Buor-Khaya Cape (YS-13). Radiocarbon ages of sinking OC range from 600 to 3900 ^{14}C-yrs BP (Table 1). There are very few other studies that have reported on radiocarbon ages of sinking POC in the Arctic. In the deep Canada basin, *Griffith et al.* [2012] report older $\Delta^{14}C$ values for sinking POC (-250 to $-300‰$; collected with sediment traps) than for particulate POC (-50 to $-200‰$; collected with submersible pump) below 1500 m depth, and *Hwang et al.* [2008] note that deep POC (3067 m) collected in sediment traps consists of aged allochthonous OC ($\Delta^{14}C$ $-220‰$) compared to more autochthonous, younger, POC at 120 m depth. The Canadian region is, however, fundamentally different with narrow shelves and a very steep continental rise, whereas the ESAS is the largest and shallowest shelf sea on Earth.

Terrestrial topsoil OC, marine OC, and ICD-OC dominate in surface particulate matter, sinking particulate matter, and surface sediment, respectively. The dual-carbon three-source mixing model we applied (Figure 3 and section 3.4) suggests an increase of the fraction ICD-OC from surface POC to sediment OC at the Lena river-influenced sites (YS-11, YS-13), while the other two stations have a more constant contribution throughout the water column and sediment (Figure 4), suggesting that the delivery of ICD-OC to shelf waters is more important in the Eastern ESAS. Topsoil OC shows an opposite pattern; for all stations, the contribution decreases with depth. The distinct contribution of topsoil OC in surface waters is likely due to its buoyant nature—being mostly organic detritus that is nonmineral associated—allowing for long-distance transport and very slow settling [*Vonk et al.*, 2010a; *Karlsson et al.*, 2011]. The relative abundance of marine OC appears highest in sinking particulate POC, particularly for the stations furthest away from the Lena River (YS-23, YS-26). Here, the average fraction of marine OC in sinking particulate POC is 21–35%, while marine OC only

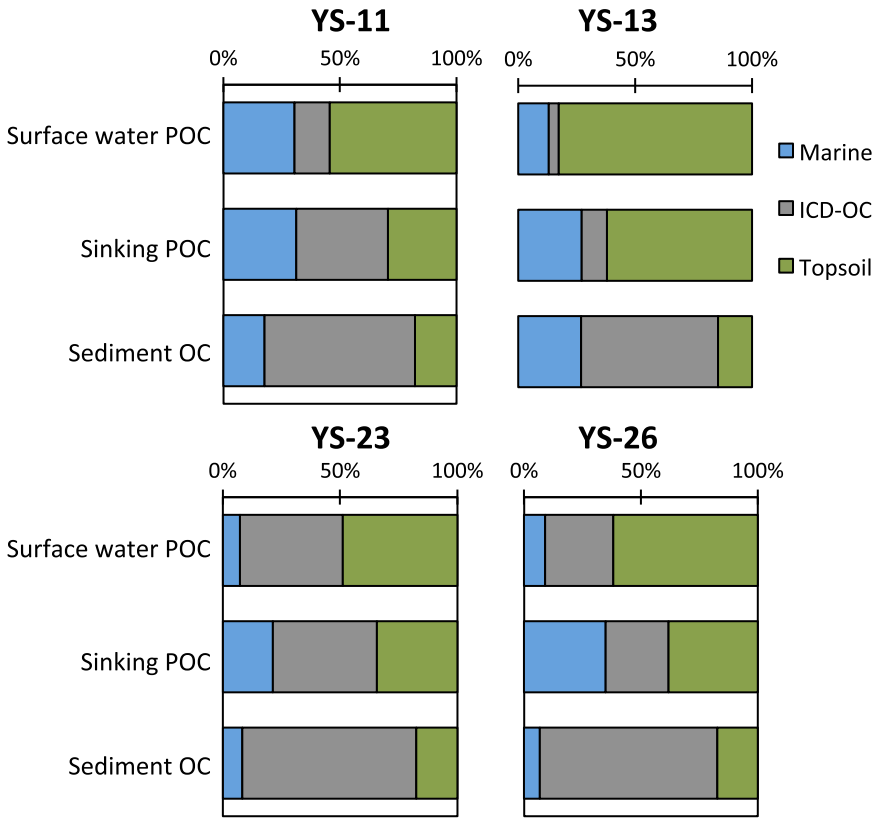

Figure 4. Monte Carlo-derived relative contribution of marine OC (blue), ICD-OC (gray), and topsoil OC (green) to surface water particulate POC, sinking particulate OC, and surface sediment OC for stations YS-11, YS-13, YS-23, and YS-26. Median values are shown, 95% confidence intervals can be found in supporting information Table S1.

contributes around 7–9% to surface particulate POC and sediment OC (Figure 4). This suggests that (i) marine OC is sufficiently heavy to settle, being ballasted by e.g., biogenic minerals, and (ii) likely more degradable than contemporary (terrestrial) OC and ICD-OC. This is supported by *Kraberg et al.* [2013] that show that horizontal transport of plankton in the Buor-Khaya Bay is limited and also suggest ongoing remineralization of phytoplankton during settling.

The radiocarbon age of recalcitrant soil OM markers in recent surface sediments increases with decreasing stratification, suggesting a greater proportion of Pleistocene OC at locations away from major rivers. Whereas bulk OC-^{14}C is inherently a mixture of material from different sources, compound-specific ^{14}C analysis can provide an unbiased signal of source-specific tracers. *Gustafsson et al.* [2011] reported ^{14}C ages of HMW *n*-alkanoic acids in Lena, Indigirka, and Kolyma river mouth sediments of 5.5 (YS-11), 9.4, and 6.0 ky BP (Δ^{14}C $-500‰$, $-693‰$, and $-532‰$), respectively. *Drenzek et al.* [2007] performed compound-specific ^{14}C analysis on *n*-alkanoic acids in near shore Beaufort Sea sediments, the only other compound-specific radiocarbon study in the High-Arctic. They found that long-chain *n*-alkanoic acids were around 6 ^{14}C-ky, which likely reflects Mackenzie River OC input mixed with erosion of Holocene sediments from the Mackenzie delta. The ESAS sediments show much older *n*-alkanoic acids; station YS-13, not far from YS-11, has a sedimentary HMW *n*-alkanoic acid ^{14}C signal of $-707‰$ while YS-23 and YS-26 show much more depleted signals ($-895‰$ and $-830‰$, respectively; Table 1).

Radiocarbon ages of recalcitrant soil markers in surface sediments increase with increasing distance from the Lena River (Figure 5a). A decrease in plant wax ^{14}C values eastward might be (partly) attributed to aging during transport. A more likely explanation, however, is an increasing contribution of preaged, Pleistocene terrestrial OC to sediment OC with increasing distance from the Lena River mouth. The Eastern ESAS coast (particularly Oyagos Yar, directly south of YS-23) experiences higher erosion rates than the Buor-Khaya Bay [*Günther et al.* 2013; *Lantuit et al.*, 2012], while the western ESAS is dominated by Lena River inflow (discharge 523 km^3/yr compared with e.g., Yana 32 km^3/yr or Indigirka 54 km^3/yr) and its currents are usually

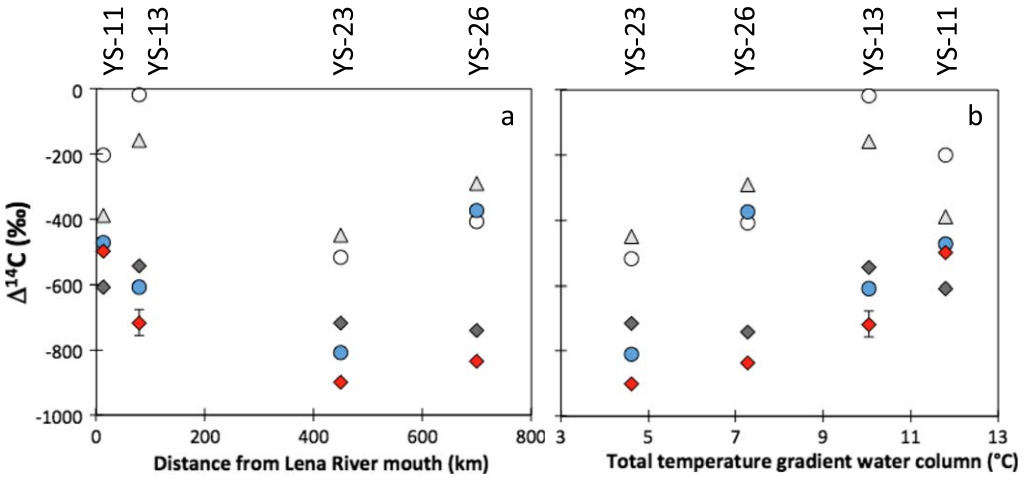

Figure 5. Bulk (OC) and molecular radiocarbon (sum of C_{24}, C_{26}, and C_{28} *n*-alkanoic acids) results for YS-11, YS-13, YS-23, and YS-26 for surface POC (open circles), sinking POC (light gray triangles), sediment POC (grey diamonds), *n*-alkanoic acids in surface POC (blue circles), and *n*-alkanoic acids in sediment OC (red diamonds), plotted as $\Delta^{14}C$ (‰), with (a) distance from Lena River mouth (km; as the crow flies), and (b) total temperature gradient in the water column (°C; from CTD), calculated as the difference between 1 m and maximum water depth. Analytical uncertainties are generally smaller than symbol size.

directed eastward (Figure 1b) [*Steele and Ermold*, 2004]. Due to dilution with other water masses, the relative impact of the Lena river gradually decreases eastward. In the summer of 2008 when the eastward freshwater flow was relatively weak, the fraction Lena river water to surface water was still estimated to be >70%, 70%, and ~50% for YS-11, YS-13, and YS-23, respectively, based on $\delta^{18}O$-derived spatial distribution maps in *Wegner et al*. [2013]. Weaker water column stratification (as reflected by the vertical temperature gradient) induced by lower freshwater inflow also correlates with older sedimentary *n*-alkanoic acid ages (Figure 5b). Hence, from west to east, sedimentary OC appears to be less affected by younger riverine (topsoil and autochthonous) organic matter, and more by older, erosion-derived organic matter. One should note that Pleistocene OC is not only delivered by coastal erosion, but is also eroded and transported from riverine catchments, as illustrated by the relatively old ^{14}C ages of bulk POC (Lena River -296 ± 68‰, n=3, *Vonk et al*. [2010b]; Kolyma River -288 ± 81‰, n=15). However, the addition of modern (topsoil and autochthonous) OC results in a much younger average age of fluvial OC compared to OC from ICD-coasts (average ^{14}C of -940 ± 84‰, n=300) [*Vonk et al*., 2012].

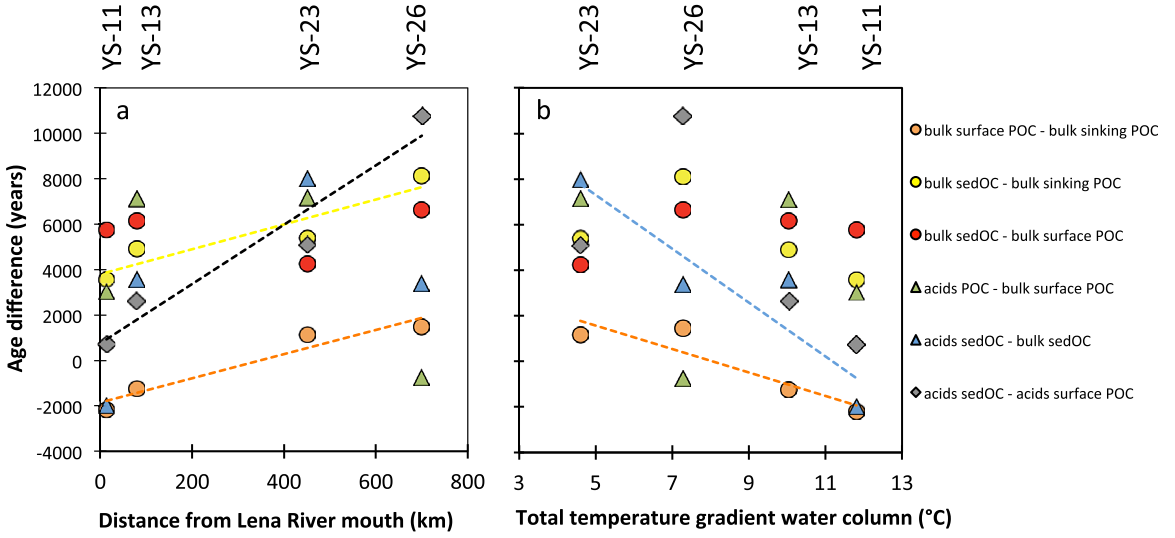

Figure 6. Shift in radiocarbon age between bulk OC (surface POC, sinking POC, and sediment OC) and HMW *n*-alkanoic acids in surface POC and sediment OC against (a) distance from the Lena River mouth, and (b) total temperature gradient water column. Age differences between bulk OC data are shown in circles, age differences between HMW *n*-alkanoic acids and bulk OC are given in triangles, and age difference between HMW *n*-alkanoic acids is given with diamonds. Dashed lines are given for trends with $R^2 > 0.8$.

Proximity to the coast, water column depth and distance from river mouths are major factors affecting the age of terrestrial OM markers in surface particulate OM. The *n*-alkanoic acid ages in surface SPM are younger than the HMW *n*-alkanoic acids in the underlying sediments, and this age difference increases (i) with increasing distance from the Lena River mouth (Figure 6a; R^2=0.91, n=4), and (ii) with decreasing stratification (Figure 6b; R^2=0.37): there is 0.7 ^{14}C-ky age difference at YS-11, 2.6–4.8 ^{14}C-ky difference for YS-13 and YS-23, respectively, and 10.8 ^{14}C-ky age discrepancy at YS-26. Additionally, small age discrepancies seem to occur at sites where OC accumulation rates, based on spatially interpolated estimates from sediment cores [*Vonk et al.*, 2012], are higher; with accumulation rates between 25 and 50 g OC/m^2/y for a 10.8 ^{14}C-ky age difference (YS-26) to accumulation rates between 75 and 100 OC/m^2/y for 0.7 ^{14}C-ky age difference (YS-11). In other words, a higher accumulation of OC suggests a stronger exchange between water column and sediments, and could explain the larger similarity in ^{14}C age of *n*-alkanoic acids in surface water and surface sediment OC. The oldest age for HMW *n*-alkanoic acids in SPM measured was almost 13 ^{14}C-ky (YS-23), and the youngest was 3.4 ^{14}C-ky (YS-26). This eastward pattern in age discrepancy can be explained by multiple reasons. First of all, station YS-26 is situated furthest away from the coast (~46km), distal from the near shore region where most coastal-erosion-derived SPM is deposited [*Are*, 1999; *Dudarev et al*., 2006; *Wegner et al*. 2005]. Long-term MERIS image analysis shows that YS-26 is located at the edge of the turbidity zone, allowing for a temporary (seasonal) decoupling between surface water OC and sediment OC depending on the spatial extent of the turbidity zone and tidal energy. *Karlsson et al*. [2011] and *Vonk et al*. [2010b] also show that mineral-associated OC from coastal erosion settles more rapidly and has less effect on the water column further away from the coast. Second, the water column depth at YS-26 is 16m, which is deeper than the lower shoreface boundary where wave impact-induced bottom resuspension of old OC might take place [*Are et al*., 2002]. This station is furthest away from fluvial input, and hence the terrestrial OM remaining in the surface water column is likely to consist mostly of younger, buoyant OC originating in surface soils. Furthermore, the ^{14}C age of sinking POC linearly decreases with overall water column depth (R^2= 0.97, including YS-4: R^2=0.71 not shown), suggesting that older, ballasted material preferentially settles out nearshore. This might suggest that fluvially derived mineral-associated (i.e., heavier), older bulk OC settles upon arrival in the Dmitry Laptev Strait (YS-23), as also suggested by the increase in age difference between sediment OC and sinking POC (Figure 6a, R^2= 0.86, n=4) with increasing distance from the Lena River mouth.

5. Conclusions

Rapid ongoing warming in the East-Siberian Arctic impacts multiple environmental factors that drive the fate of OC from thawing permafrost. Bulk and molecular radiocarbon analyses along with end-member mixing analyses shows that old OC released from thawing permafrost dominates the region, and is increasingly abundant in sediments with increasing distance from the Lena River. Old OC, however, seems to settle rapidly and only dominates the water column in shallow nearshore regions. Settling also appears to be the main transport mechanism for marine OC, yet this OC is subject to significant degradation during settling. Contemporary terrestrial OC originating in topsoils is abundant in surface waters and appears to be most widely dispersed by horizontal transport by virtue of its buoyant nature. These findings illustrate that different OC sources exhibit fundamentally different behavior upon release or production in the coastal environment. Relative to topsoil and marine OC, which appears susceptible to degradation, ICD-OC that is released into coastal water seems destined for sediment burial. While bearing in mind that this study does not include greenhouse gas emission from thawing permafrost prior to its coastal introduction (i.e., on land, in aquatic systems, and on coastal slopes), our data might suggest that the climate feedback potential of permafrost OC that is released onto the ESAS is limited.

Acknowledgments

We would like to acknowledge financial support from the Knut and Alice Wallenberg foundation, the Nordic Council of Ministers (TRI-DEFROST), the Swedish Research Council (621.2004.4039 and 621.2007.4631), The Netherlands Organization for Scientific Research (grants 825.10.022 and 863.12.004), the Government of the Russian Federation (grant 2013-220-04–157), President Grants for Government Support of Young Scientists of the Russian Federation (MK-2575.2014.5) and the Russian Foundation of Basic Research. Furthermore, we would like to thank the scientific crew of ISSS-08, Daniel Montlucon and Thomas Blattmann (ETH, Geological Institute), Cameron McIntyre and Lukas Wacker (ETH-LIP), and the staff of NOSAMS. Data are available through the Bolin Centre database (www.bolin.su.se/data).

References

Andersson, A. (2011), A systematic examination of a random sampling strategy for source apportionment calculations, *Sci. Total Environ.*, *412–413*, 232–238.

Are, F. E. (1999), The role of coastal retreat for sedimentation in the Laptev Sea, in *Land-ocean Systems in the Siberian Arctic: Dynamics and History*, edited by H. Kassens et al., pp. 287–295, Springer, Berlin.

Are, F.E. et al., (2002), Comparative shoreface evolution along the Laptev Sea coast, *Polarforschung*, *70*, 135–150.

Cavalieri, D. J., and C. L. Parkinson (2012), Arctic sea ice variability and trends, 1979–2010, *The Cryosphere 6*, 881–889, doi:10.5194/tc-6-881-2012.

Charkin, A.N. et al. (2011), Seasonal and interannual variability of sedimentation and organic matter distribution in the Buor-Khaya Gulf: the primary recipient of input of Lena River and coastal erosion in the Southeast Laptev Sea, *Biogeosciences*, *8*, 2581–2594, doi:10.5194/bg-8-2581-2011.

Doerffer, R., and H. Schiller (2007), The MERIS Case 2 water algorithm, *Int. J. Remote Sens.*, *28*, 517–535.

Drenzek, N. J. et al. (2007), Constraints on the origin of sedimentary organic carbon in the Beaufort Sea from coupled molecular 13C and 14C measurements, *Mar. Chem.*, *103*, 146–162, doi:10.1016/j.marchem.2006.06.017.

Dudarev, O. V. et al. (2006), Deposition settings on the continental shelf of the East Siberian Sea [translated into English], *Trans. Russian Acad. Sci.*, *409*(6), 822–827.

Eglinton, G., and R. J. Hamilton (1967), Leaf epicuticular waxes, *Science*, *156*, 1322–1335.

Eglinton, T. I., et al. (1996), Gas chromatographic isolation of individual compounds from complex matrices for radiocarbon dating, *Anal. Chem.*, *68*, 904–912.

Feng, X., et al. (2013), Differential mobilization of terrestrial carbon pools in Eurasian Arctic river basins, *Proc. Natl. Acad. Sci. U. S. A.*, *110*(35), 14,168–14,173, doi:10.1073/pnas.1307031110.

Francis, O. P., G. G. Panteleev, and D. E. Atkinson (2011), Ocean wave conditions in the Chukchi Sea from satellite and in situ observations, *Geophys. Res. Lett.*, *38*, L24610, doi:10.1029/2011GL049839.

Griffith, D.R., et al. (2012), Carbon dynamics in the western Arctic Ocean: insights from full-depth carbon isotope profiles of DIC, DOC, and POC, *Biogeosciences*, *9*, 1217–1224, doi:10.5194/bg-9-1217-2012.

Grigoriev, M. N. (1993), *Cryomorphogenesis of the Mouth Area of the Lena River, Yakutsk*, [in Russian], pp. 1–176, Inst. of Permafrost Study of the Siberian Branch of the Russian Acad. of Sci., Yakutsk, Russian Federation.

Grigoriev, M. N., et al. (2004), Organic carbon input to the Arctic Seas through coastal erosion, in *Organic Carbon Cycle in the Arctic Ocean: Present and Past*, edited by R. Stein and R. W. Macdonald, pp. 41–47, Springer, Berlin.

Günther, F. et al. (2013), Short- and long-term thermo-erosion of ice-rich permafrost coasts in the Laptev Sea region, *Biogeosciences*, *10*, 4297–4318, doi:10.5194/bg-10-4297-2013.

Gustafsson, Ö. et al. (2004), Evaluation of the collection efficiency of upper ocean sub-photic-layer sediment traps: A 24-month in situ calibration in the open Baltic Sea using ^{234}Th, *Limnol. Oceanogr. Methods*, *2*, 62–74.

Gustafsson, Ö. et al. (2011), Widespread release of old carbon across the Siberian Arctic echoed by its large rivers, *Biogeosciences*, *8*, 1737–1743, doi:10.5194/bg-8-1737-2011.

Gustafsson, Ö. et al. (2013), An assessment of upper ocean carbon and nitrogen export fluxes on the boreal continental shelf: A 3-year study in the open Baltic Sea comparing sediment traps, ^{234}Th proxy, nutrient, and oxygen budgets, *Limnol. Oceanogr. Methods*, *11*, 495–510, doi:10.4319/lom.2013.11.495.

Hansell, D., and J. Newton (1994), Design and evaluation of a swimmer-segregating particle interceptor trap, *Limnol. Oceanogr.*, *39*, 1487–1495, doi:10.4319/lo.1994.39.6.1487.

Hedges, J. I., R. G. Keil, and R. Benner (1997), What happens to terrestrial organic matter in the ocean? *Org. Geochem.*, *27*, 195–212.

Heim, B., et al. (2013), Ocean colour remote sensing in the Southern Laptev Sea: Evaluation and applications, *Biogeosci. Discuss.*, *10*, 3849–3889. doi:10.5194/bgd-10-3849-2013.

Höfle, S., J. Rethemeyer, C. W. Mueller, and C. John (2013), Organic matter composition and stabilization in a polygonal tundra soil of the Lena Delta, *Biogeosciences*, *10*, 3145–3158, doi:10.5194/bg-10-3145-2013.

Holmes, R. M., et al. (2012), Seasonal and annual fluxes of nutrients and organic matter from large rivers to the Arctic Ocean and surrounding seas, *Estuaries Coasts*, *35*, 369–382, doi:10.1007/s12237-011-9386-6.

Hugelius, G., et al. (2014), Improved estimates show large circumpolar stocks of permafrost carbon while quantifying substantial uncertainty ranges and identifying remaining data gaps, *Biogeosci. Discuss.*, *11*, 4771–4822, doi:10.5194/bgd-11-4771-2014.

Huguet, C., et al. (2008), Selective preservation of soil organic matter in oxidized marine sediments (Madeira Abyssal Plain), *Geochim. Cosmochim. Acta*, *72*, 6061–6068, doi:10.1016/j.gca.2008.09.021.

Hwang, J., et al. (2008), Lateral organic carbon supply to the deep Canada Basin, *Geophys. Res. Lett.*, *35*, L11607, doi:10.1029/2008GL034271.

IPCC (2013), Climate Change 2013: The physical science basis, Working group I contribution to the fifth assessment report on the intergovernmental panel on climate change, Cambridge Univ. Press, U. K.

Jeffries, M.O., J. A. Richter-Menge, and J. E. Overland (Eds.) (2013), Arctic Report Card 2013. [Available at http://www.arctic.noaa.gov/reportcard.]

Jorgenson, M. T., Y. L. Shur, and E. R. Pullman (2006), Abrupt increase in permafrost degradation in Arctic Alaska, *Geophys. Res. Lett.*, *33*, L02503, doi:10.1029/2005GL024960.

Karlsson, E. S., et al. (2011), Carbon isotopes and lipid biomarker investigation of sources, transport and degradation of terrestrial organic matter in the Buor-Khaya Bay, SE Laptev Sea, *Biogeosciences*, *8*, 1865–1879, doi:10.5194/bg-8-1865-2011.

Keil, R. G., et al. (1994), Mineralogical and textural controls on the organic composition of coastal marine sediments: Hydrodynamic separation using SPLITT-fractionation, *Geochim. Cosmochim. Acta*, *58*, 879–893.

Kraberg, A. C., et al. (2013), Phytoplankton community structure in the Lena Delta (Siberia, Russia) in relation to hydrography, *Biogeosciences*, *10*, 7263–7277, doi:10.5194/bg-10-7263-2013.

Kuptsov, V. M., and A. P. Lisitsin (1996), Radiocarbon of Quaternary along shore and bottom deposits of the Lena and the Laptev Sea sediments, *Mar. Chem.*, *53*, 301–311.

Lantuit, H., et al. (2011), Coastal erosion dynamics on the permafrost-dominated Bykovsky Peninsula, north Siberia, 1951–2006, *Polar Res.*, *30*, 7341, doi:10.3402/polar.v30i0.7341.

Lantuit, H., et al. (2012), The Arctic coastal dynamics database: A new classification scheme and statistics on arctic permafrost coastlines, *Estuaries Coasts*, *35*, 383–400.

Nicolsky, D. J., et al., (2012), Modeling sub-sea permafrost in the east Siberian Arctic shelf: The Laptev sea Region, *J. Geophys. Res.*, *117*, F03028, doi:10.1029/2012JF002358.

Örek, H., et al. (2013), Contribution to a bio-optical model for remote sensing of Lena River water, *Biogeosciences*, *10*, 7081–7094, doi:10.5194/bg-10-7081-2013.

Peterson, W., and H. Dam (1990), The influence of copepod swimmers on pigment fluxes in brine-filled vs ambient seawater-filled sediment traps, *Limnol. Oceanogr.*, *35*, 448–455, doi:10.4319/lo.1990.35.2.0448.

Pipko I. I., I. P. Semiletov, and S. P. Pugach (2005), The carbonate system of the East Siberian Sea waters, *Dokl. Earth Sci.*, *402*(4), 624–627.

Pipko I. I., et al. (2011), Interannual variability of air-sea CO_2 fluxes and carbon system in the East Siberian Sea, *Biogeosciences*, *8*, 1987–2007, doi:10.5194/bg-8-1987-2011.

Rachold, V., and H.-W. Hubberten (1999), Carbon isotope composition of particulate organic material in East Siberian rivers, in *Land-Ocean Systems in the Siberian Arctic: Dynamics and History*, edited by H. Kassens et al., pp. 223–238, Springer, Berlin.

Rachold, V., et al. (2004), Modern terrigenous organic carbon input into the Arctic Ocean, in *The Organic Carbon Cycle in the Arctic Ocean*, edited by R. Stein and R. W. Macdonald, pp. 33–35, Springer, Berlin.

Sánchez-García, L., et al. (2011), Inventories and behavior of particulate organic carbon in the Laptev and East Siberian seas, *Global Biogeochem. Cycles*, *25*, GB2007, doi:10.1029/2010GB003862.

Sánchez-García, L., et al. (2014), Characterization of three regimes of collapsing Arctic ice complex deposits on the SE Laptev Sea coast using biomarkers and dual carbon isotopes, *Permafrost Periglac.*, *25*, 172–183, doi:10.1002/ppp.1815.

Semiletov, I. P. (2013), Space-time dynamics of carbon and environmental parameters related to carbon dioxide emissions in the Buor-Khaya Bay and adjacent part of the Laptev Sea, *Biogeosciences*, *10*, 5977–5996, doi:10.5194/bg-10-5977-2013.

Semiletov, I. P., and Ö. Gustafsson (2009), East Siberian Shelf study alleviates scarcity of observations, *EOS Trans. AGU*, *90*, 145–146, doi:10.1029/2009EO170001.

Semiletov, I. P. (1999a), On aquatic sources and sinks of CO_2 and CH_4 in the Polar Regions, *J. Atmos. Sci.*, *56*, 286–306.

Semiletov, I. P. (1999b), Destruction of the coastal permafrost ground as an important factor in biogeochemistry of the Arctic Shelf waters [translated into English], *Trans. (Dokl.) Russian Acad. Sci.*, *368*, 679–682.

Semiletov, I. P., et al. (2012), On carbon transport and fate in the East Siberian Arctic land-shelf-atmosphere system, *Environ. Res. Lett.*, *7*, 13 pp., doi:10.1088/1748-9326/7/1/015201.

Shakhova, N., et al. (2014), Ebullition and storm-induced methane release from the East Siberian Arctic Shelf, *Nat. Geosci.*, *7*, 64–70, doi:10.1038/ngeo2007.

Sheesley, R. J., A. Andersson, and Ö. Gustafsson (2011), Source characterization of organic aerosols using Monte Carlo source apportionment of PAHs at two South Asian receptor sites, *Atmos. Environ. 45*, 3874–3881.

Smith, L. C., et al. (2007), Rising minimal daily flows in northern Eurasian rivers: A growing influence of groundwater in the high-latitude hydrological cycle, *J. Geophys. Res.*, *112*, G04S47, doi:10.1029/2006JG000327.

Sorokin, Y. A., and P. Y. Sorokin (1996), Plankton and primary production in the Lena River estuary and in the South-eastern Laptev Sea, *Estuar. Coast. Shelf Sci.*, *43*, 399–418.

Steele, M., and W. Ermold (2004), Salinity trends on the Siberian Shelves, *Geophys. Res. Lett.*, *31*, L24308, doi:10.1029/2004GL021302.

Stein, R., and R. W. Macdonald (2004), *The Organic Carbon Cycle in the Arctic Ocean*, 363 pp., Springer, Berlin, Germany.

Stroeve, J. C., et al. (2014), Changes in Arctic melt season and implications for sea ice loss, *Geophys. Res. Lett.*, *41*, 1216–1225, doi:10.1002/2013GL058951.

Tarnocai, C., et al. (2009), Soil organic carbon pools in the northern circumpolar permafrost region, *Global Biogeochem. Cycles*, *23*, GB2023, doi:10.1029/2008GB003327.

Tesi, T., et al. (2014), Composition and fate of terrigenous organic matter along the land-ocean continuum in East Siberia: Insights from biomarkers and carbon isotopes, *Geochim. Cosmochim Acta*, *133*, 235–256, doi:10.1016/j.gca.2014.02.045.

Vonk, J. E., et al. (2010a), Selective preservation of old organic carbon fluvially released from sub-arctic soils, *Geophys. Res. Lett.*, *37*, L11605, doi:10.1029/2010GL042909.

Vonk, J. E., et al. (2010b), Molecular and radiocarbon constraints on sources and degradation of terrestrial organic carbon along the Kolyma paleoriver transect, East Siberian Sea, *Biogeosciences*, *7*, 3153–3166.

Vonk, J. E., et al. (2012), Activation of old carbon by erosion of coastal and subsea permafrost in Arctic Siberia, *Nature*, *489*, 137–140, doi:10.1038/nature11392.

Waite, A. M., et al. (2005), Linking ecosystem dynamics and biogeochemistry: Sinking fractionation of organic carbon in a Swedish fjord, *Limnol. Oceanogr.*, *50*(2), 658–671.

Wegner, C., et al. (2005), Seasonal variations in Arctic sediment dynamics: Evidence from 1-year records in the Laptev Sea (Siberian Arctic), *Global Planet. Change*, *48*, 126–140, doi:10.1016/j.gloplacha.2004.12.009.

Wegner, C., et al. (2013), Interannual variability of surface and bottom sediment transport on the Laptev Sea shelf during summer, *Biogeosciences*, *10*, 1117–1129, doi:10.5194/bg-10-1117-2013.

Zimov, S. A., et al. (2006), Permafrost carbon: Stock and decomposability of a globally significant carbon pool, *Geophys. Res. Lett.*, *33*, L20502, doi:10.1029/2006GL027484.